JGR Space Physics

RESEARCH ARTICLE
10.1029/2019JA027128

Ion-Neutral Collision Frequencies for Calculating Ionospheric Conductivity

A. Ieda[1]

[1]Institute for Space-Earth Environmental Research, Nagoya University, Nagoya, Japan

Key Points:
- A set of ion-neutral collision frequency coefficients for calculating the electric conductivity is summarized
- The coefficients and collision types are compared with previous studies
- The nonresonant collision is physically essential for the O_2^+-O_2 pair because the *E* region temperature is low

Correspondence to:
A. Ieda,
ieda@isee.nagoya-u.ac.jp

Citation:
Ieda, A. (2020). Ion-neutral collision frequencies for calculating ionospheric conductivity. *Journal of Geophysical Research: Space Physics*, *125*, e2019JA027128. https://doi.org/10.1029/2019JA027128

Received 5 JUL 2019
Accepted 16 DEC 2019
Accepted article online 27 DEC 2019

Abstract Molecular oxygen collides with its first positive ion in the Earth's ionosphere. The collision frequency of this particle pair is used to calculate the electric conductivity of the ionosphere. However, for this parental pair there are two collision types, resonant and nonresonant, and the selection of the collision type has differed among previous studies in calculation of conductivity. In the present study, we clarify that the nonresonant collision is physically essential for this pair because the relevant temperatures are low. That is, the peak of the ionospheric conductivity occurs at altitudes between 100 and 130 km, where the temperatures of ions and neutral particles are usually lower than 600 K, and for these temperatures nonresonant collisions are dominant. The collision frequency would be underestimated by 30% if the resonant collision was assumed at an altitude of 110 km (where the temperature is 240 K). The impact of this difference on the conductivity is estimated to be small (3%), primarily because molecular nitrogen is much more abundant than molecular oxygen. Although we have confirmed that the nonresonant collision is essential, we also include the resonant type, primarily in case of possible elevated temperature events. A set of ion-neutral collision frequency coefficients for calculating the conductivity is summarized, including other particle pairs, in the Appendices. Small corrections to the traditional coefficients are made.

Plain Language Summary The Earth's ionosphere is the region between altitudes of 60 and 800 km. The ionosphere consists of plasma, that is, ions and electrons, collocated with a neutral atmosphere. Collisions between plasma and neutral atoms and molecules, such as oxygen, create an electric current. The frequencies of these collisions need to be known to calculate the electric conductivity in the ionosphere. In this study, we summarize a set of collision frequencies for calculating the electric conductivity. In particular, we clarify that the nonresonant type of collision is essential between molecular oxygen and molecular oxygen ions because the temperature is low at altitudes between 100 and 130 km, where the peak of the ionospheric current is located.

1. Introduction

The Earth's ionosphere is a region of weakly ionized plasmas that begins at an altitude of approximately 60 km (e.g., Brekke, 2013). In the ionosphere, the electric current perpendicular to the magnetic field is mostly concentrated in the E region at altitudes between 90 and 150 km. The electric current arises from different velocities between ions and electrons. The different velocities are caused by the collisions with neutral molecules and atoms ("neutrals" hereinafter). Electron-neutral collisions are less important because electrons are strongly bound to the magnetic field. It is ion-neutral collisions that dominate the electric current and conductivity. The dominant ions are NO^+, O_2^+, and O^+, and the dominant neutrals are N_2, O_2, and O.

There are two types of collisions between ions and neutrals: nonresonant electric-polarization collisions and resonant charge-exchange collisions (Dalgarno et al., 1958; Dalgarno, 1958; Banks, 1966; Banks & Kockarts, 1973; Schunk, 1977). Nonresonant collisions are possible for all ion-neutral pairs and are caused by the polarization of a neutral particle induced by an approaching ion (Figure 1a). The resonant collisions occur between ions and their parental neutrals, such as O_2^+ and O_2, and are caused by an electron jump from the parental neutral to the ion (Figure 1b). For such parental pairs, the nonresonant collision dominates at low temperatures and the resonant collision is dominant at high temperatures.

In previous studies, it is often unclear which collision type was adopted when calculating the conductivity. The collision type adopted is at times not stated, or more often the study simply refers to textbooks such as Banks and Kockarts (1973) or Schunk and Nagy (2009) (hereinafter SN2009). Such studies implicitly assume that there is a consensus for selecting the collision type in calculations of ionospheric

©2019. American Geophysical Union. All Rights Reserved.

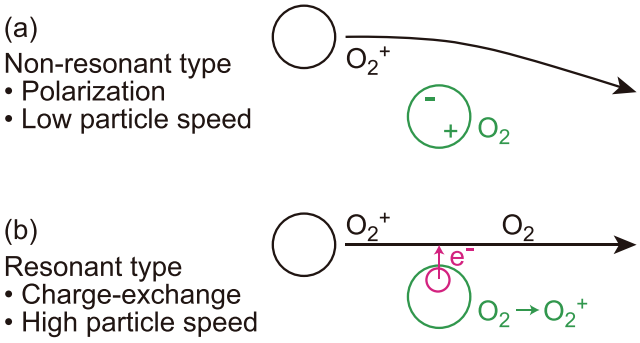

Figure 1. Two types of O_2^+-O_2 collision in the target rest frame. (a) Nonresonant type caused by the long-range polarization force. A distant collision dominant at low relative particle speeds (low temperatures). (b) Resonant type caused by electron transfer. A close collision dominant at high speeds (high temperatures).

conductivities. However, in reality, different collision types have been used in previous studies. The resonant collision is adopted for the O_2^+-O_2 pair in some studies (e.g., McGranaghan et al., 2015; Moro et al., 2016), while some other studies adopt the nonresonant collision for this pair (e.g., Brekke & Hall, 1988; Ieda et al., 2014).

The purpose of the present study is to summarize a set of collision frequencies to calculate the ionospheric conductivity. In particular, we clarify the appropriate type of O_2^+-O_2 collision to apply. We confirm that the nonresonant collision type is physically essential, while we conclude that the resonant type should also be included for robustness. The impact of the difference in O_2^+-O_2 collision type on the conductivity is investigated in a case study. We summarize the set of collision frequency coefficients in Appendix A. The coefficients are calculated in Appendices B and C, which are slightly different from the traditional values.

2. Temperature in the *E* Region

Figure 2 shows altitude profiles of a model ionospheric physical quantities above Tromsø, Norway (69.6°N, 19.2°E) at 12 UT on 30 March 2012. We selected this example event because it was geomagnetically quiet and the solar activity was moderate. That is, the 3-hr geomagnetic Kp index was [3−, 2, 1+, 1−, 1, 1−, 0, 0+] and the observed *F*10.7 index (daily 10.7-cm solar radio flux) was 110.6×10^{-22} W/m^2 Hz on this day. The 1-hr geomagnetic Dst index (World Data Center for Geomagnetism, Kyoto et al., 2015) was between −16 and 5 nT. This day was also used in our previous study (Ieda et al., 2014). Figure 2a shows the number density

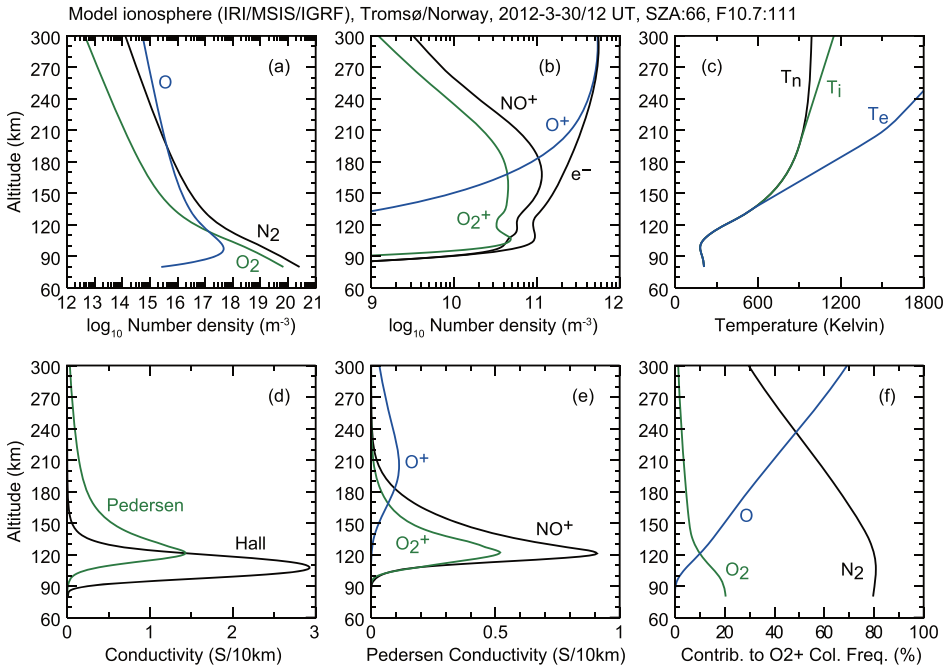

Figure 2. Altitude profiles of a model ionosphere above Tromsø, Norway (69.6°N, 19.2°E, 67° in magnetic latitude) at 12 UT on 30 March 2012. The local noon is 1047 UT. The plasma and neutral parameters are respectively obtained from the International Reference Ionosphere (IRI) 2016 model (Bilitza et al., 2017) and the Mass Spectrometer and Incoherent Scatter (MSIS) model (Picone et al., 2002). The International Geomagnetic Reference Field (IGRF-12) model (Thebault et al., 2015) is also used to calculate conductivities. Collision frequencies are calculated using the coefficients in Appendix A. (a) Number densities of neutral atmosphere (N_2, O_2, and O). (b) Number densities of ions (NO^+, O_2^+, and O^+) and electrons. (c) Neutral, ion, and electron temperatures. (d) Electric conductivity (Hall and Pedersen components). (e) Ion components (NO^+, O_2^+, and O^+) of the Pedersen conductivity. (f) Relative contribution of N_2, O_2, and O to the O_2^+ collision frequency.

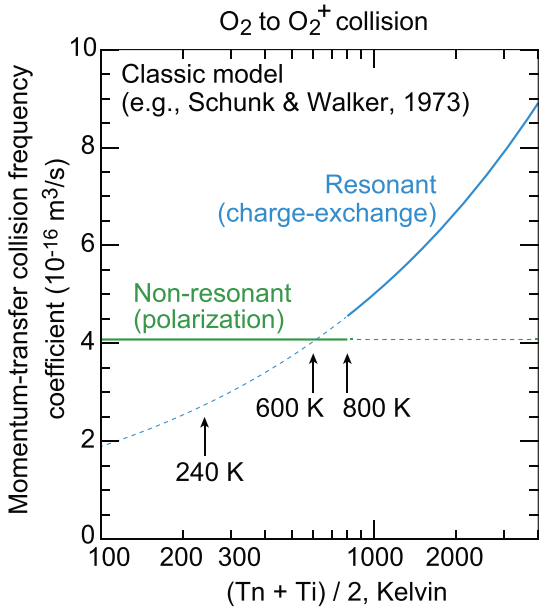

Figure 3. Classic coefficients of the O_2^+-O_2 momentum transfer collision frequency as functions of the reduced temperature. The two lines represent the nonresonant (Schunk & Walker, 1973) and resonant (Schunk & Nagy, 2009) collisions. The nonresonant (i.e., electric-polarization) collision is effective at low temperatures, and the resonant (i.e., charge-exchange) collision is effective at high temperatures (Banks, 1966; Schunk & Walker, 1973). The transition temperature has been traditionally considered to be 800 K but in reality appears to be approximately 600 K. The coefficient is 2.74 (resonant) and 4.08 (nonresonant) at 240 K, where the ratio is 2.74/4.08 ≈ 0.67.

of major neutral species (N_2, O_2, and O). Figure 2b shows the number densities of major charged species (NO^+, O_2^+, O^+, and e^-). Collisions between these neutral and charged particles create the electric conductivities.

We calculate the conductivities using a method essentially equivalent to that of Brekke and Moen (1993) and SN2009, as follows. For a charged particle species j (NO^+, O_2^+, O^+, and e^-), we define Ω_j (1/s) as the gyrofrequency and ν_j (1/s) as the momentum transfer collision frequency (sum of the collisions with N_2, O_2, and O). Using the mobility $k_j \equiv \Omega_j/\nu_j$, the conductivity for each charged species is

$$\left(\sigma_{//,j}, \sigma_{P,j}, \sigma_{H,j}\right) = \frac{en_j}{B}\left(k_j, \frac{k_j}{1+k_j^2}, \frac{k_j^2}{1+k_j^2}\right) \quad (1)$$

where //, P, and H refer respectively to the parallel, Pedersen, and Hall components. The contributions of ion species are summed so that, for example,

$$\sigma_{H,i} \equiv \sum_{j=NO^+,O_2^+,O^+} \sigma_{H,j} \quad (2)$$

where i refers to the sum of ion species. The total conductivities are

$$\left(\sigma_{//}, \sigma_P, \sigma_H\right) = \left(\sigma_{//,e} + \sigma_{//,i}, \sigma_{P,e} + \sigma_{P,i}, \sigma_{H,e} - \sigma_{H,i}\right) \quad (3)$$

where e refers to electrons.

Figure 2c shows the neutral, ion, and electron temperatures. These temperatures are close to each other in the E region, particularly in the model data. The temperatures typically increase linearly with altitude in the E region and approach 1000–2000 K in the F region (above 150-km altitude). Figure 2d shows the Hall and Pedersen conductivities, which have peaks at altitudes between 100 and 130 km, as is typical. Note also that the O_2^+ contribution to the Pedersen conductivity (Figure 2e) has a peak at altitudes lower than the Pedersen peak altitude (Figure 2d). At these altitudes below 130 km, both the neutral and ion temperatures are lower than 600 K in Figure 2c, as is typical.

3. Collision Type Depending on Temperature

Figure 3 shows the classic O_2^+-O_2 collision frequency coefficients. Two different types of collision are shown; that is, the nonresonant (Schunk & Walker, 1973) and the resonant (SN2009) types, corresponding respectively to

$$\nu(O_2^+\text{–}O_2)/[O_2] = 4.08 \qquad (T_r < 800\ \text{K, nonresonant}) \quad (4)$$

$$\nu(O_2^+\text{–}O_2)/[O_2] = 0.259\sqrt{T_r}(1-0.073\log_{10}T_r)^2 \qquad (T_r > 800\ \text{K, resonant}) \quad (5)$$

where the definitions of the physical parameters are summarized in Table A1. Note that these coefficients are not specific to the day of Figure 2 but are in fact generally applied. According to Banks (1966), the nonresonant (i.e., polarization) collision is effective below the transition temperature (800 K) and the resonant charge exchange collision is effective above the transition temperature.

However, the two lines in Figure 3 do not appear to cross at 800 K but at 617 K. This is because this traditional value of 800 K for the transition temperature was likely derived in error as follows. This temperature was likely determined in Figure 3 of Banks (1966) where the nonresonant and resonant lines appear to cross at approximately 800 K. They used a value of 1.98 for the O_2 polarizability. We calculated that this polarizability gives a transition temperature of 808 K, which is indeed approximately 800 K.

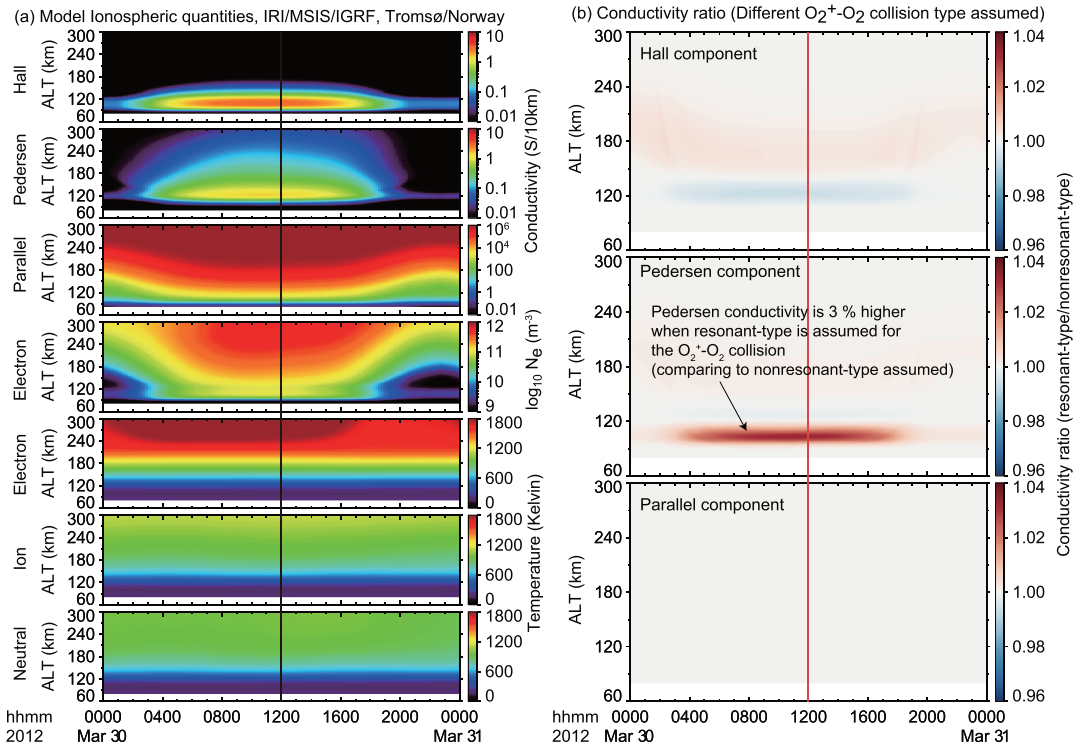

Figure 4. Time series of model ionospheric physical quantities above Tromsø, Norway (69.6°N, 19.2°E, 67° in magnetic latitude) on 30 March 2012, shown on the 10-min and 1-km grids. The vertical lines indicate 12 UT (approximately 1 hr after the local noon), corresponding to the time of Figure 2. (a) From top to bottom: calculated conductivities (Hall, Pedersen, and parallel components), model electron number density, and temperatures (electron, ion, and neutral). The O_2^+-O_2 collision type depends on the temperature. (b) Ratio of the two types of conductivities, that is, for resonant collisions and nonresonant collisions assumed for O_2^+-O_2 pairs.

In contrast, the O_2 polarizability is recognized in previous studies as approximately between 1.57 and 1.60 as listed in our Appendix B, except for their unusual value of 1.98 in their Figure 3. Moreover, the same paper (Banks, 1966) lists a different but usual value of 1.60 in their Table 1 for the O_2 polarizability. That is, Banks (1966) is not self-consistent and the use of 1.98 is likely in error. The value of 1.98 is close to the polarizability of CO instead, which is 1.97 in Table 9.10 of Banks and Kockarts (1973). Thus, it may be possible that the CO polarizability was 1.98 in an unknown reference and was used as the O_2 polarizability in Figure 3 of Banks (1966) due to confusion.

As a result of this overestimation of the O_2 polarizability, the nonresonant collision frequency and the transition temperature are overestimated in their Figure 3. The correct transition temperature should be approximately 600 K to be consistent with collision frequency coefficients listed in classic models such as Banks (1966) and Schunk and Walker (1973).

As shown in Figure 2, the neutral and ion temperatures are below approximately 600 K at the altitudes of peak conductivity. Accordingly, the nonresonant type expression in equation (4) is adequate for calculating the conductivities due to the O_2^+-O_2 collision. In particular, the relative number density of O_2^+ to other ions is highest at approximately 110-km altitude, where the temperature is 240 K in the standard atmosphere (COESA, 1976), which is much lower than 600 K. If the resonant collision was assumed at 110-km altitude, the oxygen collision frequency would be significantly (30%) underestimated.

4. Impact on the Total Conductivity

As was shown above, the resonant and nonresonant collision frequencies can be significantly different for O_2^+-O_2 pairs. We calculate the effect of this difference on the total conductivity, which also includes the contribution of other particle pairs. Figure 4a shows a 24-hr time sequence of the conductivities, electron

density, and temperatures on 30 March 2012. The vertical line indicates 12 UT, which corresponds to the instance of Figure 2. The electron density is the highest around the local noon at 1047 UT. The model electron, ion, and neutral temperatures do not show significant variation during a day when compared to the electron density variation.

Conductivities in Figure 4a were calculated by our standard method (equation (3)) using the collision frequencies (equations (A3) and (A4)), where the resonant and nonresonant type is automatically selected according to the temperature at each altitude. That is, the collision type may be different at different altitudes. In contrast, the conductivities used in Figure 4b were calculated by artificially assuming either the resonant or nonresonant O_2^+-O_2 collision at all altitudes. That is, the collision type is the same at all altitudes. We took the ratio of these resonant or nonresonant artificially-type-fixed total conductivities. Figure 4b shows the ratio of the resonant type conductivity to the nonresonant type. The red color indicates that the resonant type is higher than the nonresonant type.

The overall differences between the resonant and nonresonant O_2^+-O_2 total conductivity results are small (at most 3%) in Figure 4b, primarily because N_2 is typically four times more abundant than O_2 (Figures 2a and 2f). Accordingly, the O_2^+-O_2 collision typically contributes at most approximately 20% to the total conductivity. In addition, the number density of O_2^+ is at most comparable to NO^+ (Figures 2b and 2e) during quiet intervals, and thus, the O_2^+-O_2 collision contributes at most approximately 10%. Thus, the 30% underestimation of the O_2^+-O_2 collision frequency coefficient results in an impact to the total conductivity by at most approximately 3%. The maximum difference in this particular case is 3%, which would be typical during the daytime for quiet intervals.

We see that the difference is mostly in the Pedersen component (Figure 4b) in the lower *E* region at altitudes between 95 and 115 km during daytime. The altitude range is limited because the O_2^+ composition ratio is high only at these altitudes (Figure 2b), presumably as the result of Chapman-type solar photoionization. The Pedersen conductivity has a peak at 120-km altitude (Figure 2d). Below this altitude, an underestimation of the ion-neutral collision frequency corresponds to an overestimation of the Pedersen conductivity.

A weak underestimation (1%), indicated by the blue color, is seen in the Hall component (Figure 4b) near the peak Pedersen altitude (120 km), where the Hall component is sensitive to the ion-neutral collision frequency. The difference is not evident in the parallel conductivity, which is dominated by electrons.

5. Discussion

5.1. O_2^+-O_2 Collision

As detailed in section 1, two different types of O_2^+-O_2 collisions are considered in previous studies: the resonant type (e.g., McGranaghan et al., 2015; Moro et al., 2016) and the nonresonant type (e.g., Brekke & Hall, 1988; Ieda et al., 2014). In the present study, we have clarified that the nonresonant type is usually physically appropriate for O_2^+-O_2 collisions for calculating the conductivity because both the neutral and ion temperatures are usually lower than approximately 600 K near the peak conductivity altitudes.

However, the ion temperature may be unusually elevated in some occasions. In addition, while the transition temperature had been traditionally recognized as 800 K, it is clarified in the present study to be 600 K. The values of 800 and 600 K correspond respectively to altitudes of 183 and 145 km, according to the standard atmosphere (COESA, 1976). That is, the transition altitude is no more outside the E region. Thus, it is more general to also consider the resonant O_2^+-O_2 collisions.

Considering both collision types is consistent with the original proposal by Banks (1966), who used either the nonresonant or resonant coefficient depending on the temperature of interest. In this regard SN2009 is not readily clear. SN2009 lists the O_2^+-O_2 collision frequency coefficient for the case above 800 K in their Table 4.5. However, SN2009 does not explicitly give the O_2^+-O_2 coefficient for the case below 800 K; thus, their table is incomplete. Confusingly, SN2009 states that the nonresonant collision occurs between unlike particles. This statement may have been interpreted that there are no nonresonant collisions for parental pairs. Note that the O_2^+-O_2 nonresonant coefficient is explicitly listed in Schunk and Walker (1973).

We calculate and connect the O_2^+-O_2 resonant and nonresonant coefficients as follows. The nonresonant coefficient is calculated in Appendix B as

$$\nu(O_2^+\text{–}O_2)/[O_2] = 4.08 \qquad \text{(low temperature, nonresonant)} \tag{6}$$

See Table A1 for definitions of the parameters. We calculated the resonant coefficient in Appendix C as

$$\nu(O_2^+\text{–}O_2)/[O_2] = 0.262\sqrt{T_r}(1\text{–}0.0735\log_{10}T_r)^2 \qquad \text{(high temperature, resonant)} \tag{7}$$

Either the resonant or resonant coefficient was selected depending on the temperature of each data points (i.e., practically at each altitude) in classic models (Banks, 1966; Schunk & Walker, 1973).

Equivalently, we use the greater of equation (6) or (7) as

$$\nu(O_2^+\text{–}O_2)/[O_2] = \max\left(4.08, 0.262\sqrt{T_r}(1\text{–}0.0735\log_{10}T_r)^2\right) \tag{8}$$

This expression is possible because the resonant coefficient monotonically increases with temperature. That is, although we define the transition temperature as the temperature (607 K) at which equations (6) and (7) cross, the value is not necessary in the actual calculations of the conductivity.

Note that Banks (1966) emphasized that the total collision frequency is not the sum of the resonant and nonresonant frequencies. He recognized that the collision frequency is slightly enhanced (less than approximately 10%) near the transition temperature but ignored this enhancement in the final expressions. Accordingly, we simply connect equations (6) and (7) by using equation (8). Other connection methods would be possible, for example, using spline functions.

5.2. O^+-O Collision

So far we have studied the O_2^+-O_2 collision frequency in the present study. The other parental pair relevant for the ionospheric conductivity is the O^+-O collision. For this pair, the resonant collision has been traditionally assumed for calculating the conductivity, presumably because the transition temperature is relatively low (231 K based on Appendix A) and in addition this light particle pair tends to be located at high altitudes.

Although the nonresonant collision is probably always negligible in the Earth's recent ionosphere, we include it for robustness. Our expression is

$$\nu(O^+\text{–}O)/[O] = \max\left(4.01, 0.368\sqrt{T_r}(1\text{–}0.0648\log_{10}T_r)^2\right) \tag{9}$$

where we calculate the nonresonant coefficient (i.e., 4.01) in Appendix B, and the resonant coefficients in Appendix C.

6. Conclusions

Different O_2^+-O_2 collision types have been used in previous studies, often without a clear explanation for the choice. We have clarified that the nonresonant-type collision is physically essential because the temperature is usually low near the altitudes corresponding to peak conductivity. The O_2^+-O_2 collision frequency would be significantly (30%) underestimated if the resonant collision was assumed at 110-km altitude.

The impact of this difference on the total conductivity is estimated to be small because other particle pairs also contribute. The impact was expected to be at most approximately 3% during quiet daytime, and this expectation was consistent with a case study. The impact may be significantly different in other conditions, in particular in the presence of auroral precipitations. However, it is currently difficult to demonstrate this, because the O_2^+ composition ratio is unknown under active conditions.

Although the nonresonant collision is essential for the O_2^+-O_2 pair, we discussed that it is more appropriate to consider the resonant collision as well, primarily for elevated temperature cases. In addition, the transition temperature is found to be lower (600 K) than the traditionally assumed value (800 K), reducing the nonresonant domain, and thus reducing the justification for only using the nonresonant coefficients. In summary, the merged coefficient (equation (A1)) is appropriate for the O_2^+-O_2 pair.

We summarize a set of collision frequencies for calculating the ionospheric conductivity in Appendix A. We slightly correct the collision frequency coefficients of SN2009 in Appendices B and C within the classic regime constructed by Banks (1966).

Appendix A: Summary of Collision Frequency Coefficients

The coefficients of the momentum transfer collision frequency are summarized in this appendix. These coefficients are used in this study to calculate the electric conductivities in the Earth's ionosphere. Small corrections are made to traditional coefficients, as explained in Appendices B and C. The definitions of the physical parameters associated with the coefficients are listed in Table A1.

Collisions of neutral (N_2, O_2, and O) and charged (NO^+, O_2^+, O^+, and e^-) particles are assumed to be dominant in the Earth's ionosphere. There, collisions between ion and neutrals can be resonant or nonresonant. The nonresonant collision coefficients are calculated in Appendix B. The resonant collisions are calculated in Appendix C and are relevant only for parental pairs (i.e., O_2^+-O_2 and O^+-O). The parental pairs also have nonresonant coefficients. The merged coefficients of the parental pairs are concluded in section 5 to have the following forms:

$$C(O_2^+\text{–}O_2) \equiv \nu(O_2^+\text{–}O_2)/[O_2] = \max\left(4.079, 0.2617\sqrt{T_r}(1-0.07351\log_{10}T_r)^2\right) \quad \text{(A1)}$$

$$C(O^+\text{–}O) \equiv \nu(O^+\text{–}O)/[O] = \max\left(4.014, 0.3683\sqrt{T_r}(1-0.06482\log_{10}T_r)^2\right) \quad \text{(A2)}$$

where the "max" operator indicates the greater of the two coefficients (i.e., the nonresonant or resonant) for each temperature.

Using these parental-pair merged-coefficients and the unlike-pair nonresonant coefficients, the coefficients for each ion species are expressed as follows:

$$\begin{pmatrix} \nu(NO^+) \\ \nu(O_2^+) \\ \nu(O^+) \end{pmatrix} = \begin{pmatrix} 4.355 & 4.280 & 2.445 \\ 4.146 & C(O_2^+\text{–}O_2) & 2.318 \\ 6.847 & 6.661 & C(O^+\text{–}O) \end{pmatrix} \begin{pmatrix} [N_2] \\ [O_2] \\ [O] \end{pmatrix} \quad \text{(A3)}$$

Note that the number of valid significant digits of constants in equations (A1)–(A3) is at most three, although the constants are rounded to the four-digit values that we actually used in the present study. We prefer to keep the fourth digit because the constants are intermediate results before final quantities such as collision frequencies and conductivities.

The coefficients of the electron-neutral collision frequencies are adopted from SN2009 as follows:

$$\begin{aligned} \nu(e^-) = {} & 0.233\left(1-1.21\times10^{-4}T_e\right)T_e[N_2] \\ & + 1.82\left(1+3.6\times10^{-2}\sqrt{T_e}\right)\sqrt{T_e}[O_2] \\ & + 0.89\left(1+5.7\times10^{-4}T_e\right)\sqrt{T_e}[O] \end{aligned} \quad \text{(A4)}$$

Table A1
Definitions of the Physical Parameters Associated With Collision Frequency

Physical parameters	Definition
$[N_2]$, $[O_2]$, $[O]$ $(1/m^3)$	Number density of neutral molecular nitrogen, molecular oxygen, and atomic oxygen
ν $(10^{-16}/s)$	Momentum transfer collision frequency
C $(10^{-16}\ m^3/s)$	Coefficient of momentum transfer collision frequency
T_e, T_i, T_n (K)	Temperatures of electrons, ions, and neutral gases
T_r (K)	Reduced temperature $(T_n + T_i)/2$

Note. "Collision frequency" in the present study refers to the momentum-transfer collision frequency for momentum transfer from neutral particles. The laboratory frame is used throughout the present study except when the center-of-mass frame is explicitly stated.

Appendix B: Nonresonant Collision Frequency Coefficients

Nonresonant electric-polarization collisions occur between all ion-neutral pairs. The coefficients of the momentum transfer collision frequency for this type are calculated in this appendix and small corrections are made to traditional coefficients.

We calculate the coefficients using the classic method (Banks, 1966; SN2009), which uses the nonresonant collision cross section form derived by Dalgarno et al. (1958). SN2009 calculated the nonresonant collision frequency coefficients using their equation 4.88 with neutral gas polarizabilities in their Table 4.1. However, their results do not perfectly match our results for the following reasons.

The ion-neutral nonresonant collision frequency (equation 4.88 of SN2009) is

$$\nu_{in} = 2.21\pi e\sqrt{\frac{\gamma_n}{\mu_{in}}}n_n\frac{m_n}{m_i+m_n} \tag{B1}$$

where we believe that the following definitions are appropriate: collision frequency ν_{in} (1/s); fundamental charge e (esu) = 4.803205×10^{-10}; neutral gas polarizability γ_{n} (cm^3); neutral number density, n_{n} (cm^{-3}), mass of ions and neutrals m_{i} (g), m_{n} (g), and reduced mass $\mu_{in} = m_i m_n/(m_i+m_n)$.

We translate this equation into

$$\nu_{in}(1/\mathrm{s}) = 25.879\times10^{-16}\sqrt{\frac{\alpha_0}{\mu_{in}}}n_n\frac{m_n}{m_i+m_n} \tag{B2}$$

where the units are changed to neutral gas polarizability α_0 (10^{-24} cm^3), neutral number density n_{n} (m^{-3}), and mass in the unified atomic mass unit (u) (i.e., N_2: 28, NO^+: 30, $O_2{}^+/O_2$: 32, O^+/O: 16). For clarification, the conversion from equation (B1) to equation (B2) includes

$$\sqrt{\frac{\gamma_n(\mathrm{cm}^3)}{\mu_{in}(\mathrm{g})}}n_n\left(\mathrm{cm}^{-3}\right) = \sqrt{\frac{10^{-24}\alpha_0(10^{-24}\mathrm{cm}^3)}{\mathrm{m_u(g)}\mu_{in}(\mathrm{u})}}10^{-6}n_n\left(\mathrm{m}^{-3}\right) = \frac{10^{-6}}{\sqrt{1.660539}}\sqrt{\frac{\alpha_0}{\mu_{in}}}n_n \tag{B3}$$

where m_{u} (g) = 1.660539×10^{-24} is the unified atomic mass constant. Equation (B2) is equivalent to equation 9 of Banks (1966) and equation 9.73 of Banks and Kockarts (1973), where the center of mass frame is used and the neutral number density is in cubic centimeters.

Equation (B2) indicates that the nonresonant coefficient of a particle pair depends on the neutral gas polarizability. The polarizabilities and resultant nonresonant coefficients used in the present study are shown in Table B1, along with values from previous studies. There are some differences between the present results, SN2009, and Schunk and Walker (1973).

The O_2-associated coefficients are slightly smaller in SN2009 (4.27, 6.64) than in Schunk and Walker (1973) (4.28, 6.66). Since the polarizabilities are the same between them, this is an inconsistency. SN2009 states that

Table B1
Coefficients of the Ion-Neutral Nonresonant Momentum Transfer Collision Frequency

	Polarizability $\alpha_0(10^{-24}\mathrm{cm}^3)$	Coefficient of nonresonant collision frequency $C(10^{-16}\mathrm{m}^3/\mathrm{s})$		
Reference	N_2, O_2, O	NO^+—(N_2,O_2,O)	$O_2{}^+$—(N_2,O_2,O)	O^+—(N_2,O_2,O)
Present study	1.76, 1.59, 0.77	4.36, 4.28, 2.45	4.15, 4.08, 2.32	6.85, 6.66, 4.01
Schunk and Nagy (2009) Tables 4.1 and 4.4	1.76, 1.60[a], 0.77	4.34, 4.27, 2.44	4.13, —, 2.31	6.82, 6.64, —
Schunk and Walker (1973) appendix	1.76, 1.60, 0.77	4.34, 4.28, 2.44	4.13, 4.08, 2.31	6.82, 6.66, —
Banks and Kockarts (1973) Table 9.10	1.76, 1.59, 0.79	—, —, —	—, —, —	—, —, —
Banks (1966) Tables 1 and 10	1.76, 1.60[b], 0.89[c]	—, —, —	—, 4.1, —	—, —, 4.3[d]

Note. The coefficients depend on the neutral gas polarizabilities. Dashes indicate that coefficients were not explicitly listed in the corresponding references.
[a]Typo. Should be 1.59. [b]Their Figure 3 uses 1.98 instead. [c]Different from their reference. Should be 0.77. [d]Error due to (c). Should be 4.0.

Table B2
Supplemental Neutral Gas Polarizabilities

Reference	Polarizability $\alpha_0(10^{-24}\text{cm}^3)$		
	N_2	O_2	O
Hasted (1964)[a] Appendix 9	1.74	1.57	—
Hirschfelder et al. (1964) Table 13.2-3	1.76	1.60	—
Dalgarno (1961)[a] Table 3	—	—	0.77
Dalgarno and Parkinson (1959) Table 2	—	—	0.89
Alpher and White (1959) Table 1	—	—	0.77

Note. Dashes indicate that polarizabilities were not listed in the corresponding references.
[a]Referred by Banks (1966).

they use the O_2 polarizability (1.60) in their Table 4.1, which refers to Banks and Kockarts (1973), where the polarizability is in fact 1.59. Thus, the 1.60 in SN2009 is likely a typo and it should have been 1.59 (footnote (a) in Table B1 caption).

We adopt the set of polarizabilities that is likely actually used by SN2009. However, our results still do not match SN2009 (e.g., 4.36 and 4.34 for the NO^+-N_2 pair). We can marginally reproduce the coefficients in SN2009 only if the factor 25.879 in equation (B2) was approximately 25.79. Neither 25.78 nor 25.80 lead to a good reproduction. We noticed that the use of the proton mass (1.672622×10^{-24} g) instead of the unified atomic mass constant in equation (B2) results in the factor of 25.79. This is one possible interpretation for the remaining small differences between our results and SN2009. The neutron mass (1.674927×10^{-24} g) results in the factor of 25.77 and did not provide good results.

B.1. Supplemental Clarification of Polarizability

Regarding the polarizabilities α_0 (10^{-24} cm^3) listed in Table B1, footnotes (a) and (b) have been already explained respectively in this appendix and in section 3. Here we make supplemental clarifications for footnotes (c) and (d) by reviewing supplemental references listed in Table B2.

Banks and Kockarts (1973) does not include references, and Banks (1966) includes referencing errors as follows. Table 1 of Banks (1966) refers to Hasted (1964) and Dalgarno (1961) for polarizabilities. However, the N_2 and O_2 values are not listed in Dalgarno (1961), and are 1.74 and 1.57 respectively on page 506 of Hasted (1964), which are different from the values in Banks (1966) (1.76 and 1.60). We coincidentally noticed that Hirschfelder et al. (1964) lists these values on page 950, which may be what Banks (1966) intended to refer to. The O_2 polarizability of 1.59 in Banks and Kockarts (1973) includes no reference, but would be acceptable because it is between 1.57 and 1.60.

The O polarizability does not appear to be listed in Hirschfelder et al. (1964) nor Hasted (1964), and is listed in Table 3 of Dalgarno (1961) as $5.2 \times 0.148 \approx 0.77$. Thus, the Banks (1966) value of 0.89 does not exist in their references, for which we provide the following possible explanation. We coincidentally noticed that Dalgarno and Parkinson (1959) lists two different values for the O polarizability in their Table 2: their theoretical result of 0.89 and an experimental result of 0.77 by Alpher and White (1959). Dalgarno and Parkinson (1959) expected that their theoretical value of 0.89 was overestimated, and in fact Dalgarno (1961) lists only the experimental value of 0.77 as the "recommended" value, which was referenced as 0.89 by Banks (1966). That is, Banks (1966) likely uses the unrecommended value out of confusion.

Moreover, the concluding Table 10 of Banks (1966) is not self-consistent regarding the O^+-O collision. That is, the transition temperature can be calculated using their listed nonresonant and resonant coefficients to be 301 K but is concluded to be $470/2 = 235$ K instead. This traditional 235 K is very close to our model (231 K based on Appendix A), which is supposed to be correct. Accordingly, one possible interpretation of the inconsistency is that they had two different nonresonant collision frequency coefficients. That is, they calculated and listed the transition temperature using an unlisted practically-correct coefficient (~4.0) that is based on the correct polarizability (0.77), but in confusion they listed the incorrect coefficient (4.3 in Table B1) that is based on the incorrect polarizability (0.89).

These errors in Banks (1966) were presumably noticed and improved by Banks and Kockarts (1973), although they have no explanation nor references for their Table 9.10. Schunk and Walker (1973) follow Banks (1966) except that they use 0.77 for the O polarizability presumably because they noted the error. SN2009 intends to follow Banks and Kockarts (1973) except still using 0.77 for the O polarizability. Accordingly, we have followed SN2009 in selection of the O polarizability.

Appendix C: Resonant Collision Frequency Coefficients

The resonant charge-exchange collision occurs between ions and their parental neutrals. The O_2^+-O_2 and O^+-O pairs are relevant to the electric conductivity in the Earth's ionosphere. The coefficients of the

Table C1
Input Parameters of the Average Resonant Charge Exchange Cross Section

Collision Pair	O_2^+-O_2	O^+-O
Cross-Section Parameter	$A_0 = 5.37$, $B_0 = 0.54$	$A_0 = 5.59$, $B_0 = 0.475$
Original Source	Amme and Utterback (1964)	Knof et al. (1964)
Source in Banks (1966)	Table 6	Table 4

Note. These parameters are used in equation (C1).

momentum transfer collision frequency for this type are calculated in this appendix and small corrections are made to traditional coefficients.

We calculate the coefficients using the classic method (equations 25, 26, and 28 of Banks, 1966), which is equivalent to equation 4.151 of SN2009. Our resultant coefficients are slightly different from those of the classic models (Banks, 1966; Banks & Kockarts, 1973; SN2009). However, the coefficients should be essentially the same because the same formula (Dalgarno, 1958) and parameters (Table C1) were adopted for the charge-exchange cross section. To confirm this, we clarify the causes of the differences as follows.

The parameters in Table C1 are used in the average resonant charge-exchange cross section that is approximated in equation 26 of by Banks (1966) as

$$Q_E(\mathrm{cm}^2) = [(\mathrm{A}_0 + \mathrm{R}_{2T}\mathrm{B}_0) - \mathrm{B}_0 \log_{10}(2T_r)]^2 \tag{C1}$$

where $R_{2T} = 3.96$.

The resonant momentum transfer collision frequency in the center-of-mass (CM) frame is

$$\nu_{\mathrm{CM}} = \mathrm{f}_0 \sqrt{2T_r} 2 Q_E n_n \tag{C2}$$

where $\mathrm{f}_0 \equiv \frac{4}{3}\sqrt{\frac{8k_B}{\pi m}}$ is a factor, where $\mathrm{k_B}$ is the Boltzmann constant (1.380649×10^{-16} erg/K), and m (g) is explained by Banks (1966) as "the ion or neutral particle mass". We recognize this m (g) as being twice of the reduced mass and approximate it for simplicity as the neutral mass. We use the unified atomic mass constant 1.660539×10^{-24} g multiplied by 32 (O_2^+-O_2 collision) or 16 (O^+-O collision).

Comparing equations (C1) and (C2), the momentum transfer collision frequency coefficient can be expressed as

$$\begin{aligned} \nu_{\mathrm{CM}}/n_n &= \mathrm{f}_0 \sqrt{2T_r} 2 [(\mathrm{A}_0 + \mathrm{R}_{2T}\mathrm{B}_0) - \mathrm{B}_0 \log_{10}(2T_r)]^2 \\ &= 2\mathrm{f}_0 \sqrt{2}\sqrt{T_r} [(\mathrm{A}_0 + (\mathrm{R}_{2T} - \log_{10} 2)\mathrm{B}_0) - \mathrm{B}_0 \log_{10} T_r]^2 \end{aligned} \tag{C3}$$

C.1. Banks Output Style

Banks and Kockarts (1973) lists the coefficients as functions of $2T_r$ in the center-of-mass frame as

$$\nu_{\mathrm{CM}}/n_n = \mathrm{f}_{\mathrm{BK}} \sqrt{2T_r} [\mathrm{A}_{\mathrm{BK}} - \mathrm{B}_{\mathrm{BK}} \log_{10}(2T_r)]^2 \tag{C4}$$

Comparing with equation (C3), the constants are

Table C2
Constants for Resonant Collision Frequency Coefficients in Banks Output Style

	Constants f_{BK}, A_{BK}, B_{BK}	
Collision Pair	O_2^+-O_2	O^+-O
Present Study	0.0034, 10.6, 0.76	0.0049, 10.6, 0.67
Banks and Kockarts (1973), Table 9.13	0.0034, 10.6, 0.76	0.0048, 10.6, 0.67
Banks (1966), Table 10	0.0034, 10.6, 0.76	0.0047, 10.5, 0.67

Note. The constants are defined in equation (C5) and are used in equation (C4).

$$\begin{cases} A_{BK} = \sqrt{2}(A_0 + R_{2T}B_0) \\ B_{BK} = \sqrt{2}B_0 \\ f_{BK} = f_0 \end{cases} \quad \text{(C5)}$$

Using the cross-section parameter in Table C1, our results in this Banks output style are

$$\nu_{CM}(O_2^+\text{–}O_2)/[O_2] = 3.4297\cdot10^{-3}\sqrt{2T_r}(10.618\text{–}0.76368\log_{10}(2T_r))^2 \quad \text{(C6)}$$

$$\nu_{CM}(O^+\text{–}O)/[O] = 4.8503\cdot10^{-3}\sqrt{2T_r}(10.566\text{–}0.67175\log_{10}(2T_r))^2 \quad \text{(C7)}$$

These results are compared in Table C2 with Banks (1966) and Banks and Kockarts (1973). Our results are very close to Banks and Kockarts (1973). We noticed that the use of the proton or neutral mass instead of the unified atomic mass constant in equation (C2) results in a perfect match. There are small differences between Banks (1966) and Banks and Kockarts (1973) for the O^+-O collision. Since Banks and Kockarts (1973) is much closer to our results, they presumably noticed and improved the errors in Banks (1966). That is, the O^+-O collision frequency is underestimated by approximately 4% at 1000 K in Banks (1966).

C.2. Schunk Output Style

SN2009 lists the coefficients as function of T_r in the laboratory (LAB) or ionospheric frame as

$$\nu_{LAB}/n_n = f_{SN}\sqrt{T_r}[1\text{–}B_{SN}\log_{10}T_r]^2 \quad \text{(C8)}$$

Equation (C3) should be multiplied by $m_n/(m_i{+}m_n) \approx 1/2$ in this frame. That is, $\nu_{LAB} \approx \nu_{CM}/2$ for the resonant charge-exchange collision. Accordingly, the constants are

$$\begin{cases} A_{SN} = A_0 + (R_{2T}\text{–}\log_{10}2)B_0 \\ B_{SN} = B_0/A_{SN} \\ f_{SN} = f_0\sqrt{2}A_{SN}^2 \end{cases} \quad \text{(C9)}$$

Using the cross-section parameter in Table C1, our results in this Schunk output style are

$$\nu_{LAB}(O_2^+\text{–}O_2)/[O_2] = 0.26173\sqrt{T_r}(1\text{–}0.073511\log_{10}T_r)^2 \quad \text{(C10)}$$

$$\nu_{LAB}(O^+\text{–}O)/[O] = 0.36834\sqrt{T_r}(1\text{–}0.064820\log_{10}T_r)^2 \quad \text{(C11)}$$

These coefficients are compared with SN2009 in Table C3. Our results slightly differ from SN2009. The SN2009 coefficients can be reproduced by starting from the Banks and Kockarts (1973) coefficients in Table C2. Thus, it is likely that SN2009 did not directly calculate the coefficients but converted the Banks and Kockarts results, which were already rounded. This is one possible interpretation why SN2009 results are slightly (<~1%) different from our results.

Table C3
Constants for Resonant Collision Frequency Coefficients in Schunk Output Style

	Constants f_{SN}, B_{SN}	
Collision pair	O_2^+-O_2	O^+-O
Present study	0.262, 0.074	0.368, 0.065
Schunk and Nagy (2009), Table 4.5	0.259, 0.073	0.367, 0.064

Note. The constants are defined in equation (C9) and are used in equation (C8).

For clarification, equations (C4) and (C8) are equivalent and are associated through $\nu_{LAB} = \nu_{CM}/2$, which can be transformed as

$$f_{SN}\sqrt{T_r}[1\text{–}B_{SN}\log_{10}T_r]^2 = f_{BK}\sqrt{2T_r}[A_{BK}\text{–}B_{BK}\log_{10}(2T_r)]^2/2 \quad \text{(C12)}$$

$$f_{SN}[1\text{–}B_{SN}\log_{10}T_r]^2 = f_{BK}\left(G^2/\sqrt{2}\right)[1\text{–}(B_{BK}/G)\log_{10}T_r]^2 \quad \text{(C13)}$$

where $G \equiv A_{BK} - B_{BK}\log_{10}2$ is a temporal constant. Accordingly, the conversion from the Banks output style to the Schunk output style is

$$\begin{cases} B_{SN} = B_{BK}/G \\ f_{SN} = f_{BK}G^2/\sqrt{2} \end{cases} \quad \text{(C14)}$$

Acknowledgments
A. I. wishes to thank M. Takeda, Y. Koyama,Y. Ogawa, and H. Shinagawa for their helpful discussions. The code for the International Reference Ionosphere (IRI) 2016 model was received from http://irimodel.org/ website. The Kp index was provided by GFZ German Research Centre for Geosciences (https://www.gfz-potsdam.de/en/kp-index/). The *F*10.7 index was provided by NOAA's NGDC (https://www.ngdc.noaa.gov/stp/solar/solar-indices.html). The Dst index was provided by the WDC for Geomagnetism, Kyoto (http://wdc.kugi.kyoto-u.ac.jp/wdc/Sec3.html). Physical constants used in the present study are based on the 2018 CODATA (committee on data for science and technology) recommended values at https://physics.nist.gov/constants and the ninth edition of the SI (international system of units) brochure (2019) at https://www.bipm.org/ website. This work was supported by JSPS KAKENHI Grant 16K05568.

References

Alpher, R. A., & White, D. R. (1959). Optical refractivity of high-temperature gases. 1. Effects resulting from dissociation of diatomic gases. *Physics of Fluids*, *2*(2), 153–161. https://doi.org/10.1063/1.1705906

Amme, R. C., & Utterback, N. G. (1964). Effects of ion beam excitation of charge transfer cross section measurements. In M. R. C. McDowell (Ed.), *Atomic Collision Processes* (pp. 847–853). Amsterdam: North-Holland publishing.

Banks, P. (1966). Collision frequencies and energy transfer—Ions. *Planetary and Space Science*, *14*(11), 1105–1122. https://doi.org/10.1016/0032-0633(66)90025-0

Banks, P. M., & Kockarts, G. (1973). *Aeronomy, Part A*. New York: Academic Press.

Bilitza, D., Altadill, D., Truhlik, V., Shubin, V., Galkin, I., Reinisch, B., & Huang, X. (2017). International Reference Ionosphere 2016: From ionospheric climate to real-time weather predictions. *Space Weather-the International Journal of Research and Applications*, *15*, 418–429. https://doi.org/10.1002/2016sw001593

Brekke, A. (2013). *Physics of the upper polar atmosphere* (2nd ed.). Heidelberg: Springer.

Brekke, A., & Hall, C. (1988). Auroral ionospheric quiet summer time conductances. *Annales Geophysicae-Atmospheres Hydrospheres and Space Sciences*, *6*(4), 361–375.

Brekke, A., & Moen, J. (1993). Observations of high-latitude ionospheric conductances. *Journal of Atmospheric and Terrestrial Physics*, *55*(11-12), 1493–1512. https://doi.org/10.1016/0021-9169(93)90126-j

COESA (1976). *U.S. standard atmosphere, 1976*. Washington, DC: U.S. Government Printing Office.

Dalgarno, A. (1958). The mobilities of ions in their parent gases. *Philosophical Transactions of the Royal Society of London. Series A, Mathematical and Physical Sciences*, *250*(982), 426–439. https://doi.org/10.1098/rsta.1958.0003

Dalgarno, A. (1961). Intermolecular potentials for ionic systems. *Planetary and Space Science*, *3*, 217–220. https://doi.org/10.1016/0032-0633(61)90248-3

Dalgarno, A., McDowell, M. R. C., & Williams, A. (1958). The mobilities of ions in unlike gases. Philosophical Transactions of the Royal Society of London. *Series A, Mathematical and Physical Sciences*, *250*(982), 411–425. https://doi.org/10.1098/rsta.1958.0002

Dalgarno, A., & Parkinson, D. (1959). The polarizabilities of atoms from boron to neon. Proceedings of the Royal Society of London. *Series A, Mathematical and Physical Sciences*, *250*(1262), 422–426. https://doi.org/10.1098/rspa.1959.0073

Hasted, J. B. (1964). *Physics of atomic collisions*. London: Butterworths.

Hirschfelder, J. O., Curtiss, C. F., & Bird, R. B. (1964). *Molecular theory of gases and liquids (Second printing, Corrected with notes added, March, 1964 ed.)*. New York: Wiley.

Ieda, A., Oyama, S., Vanhamäki, H., Fujii, R., Nakamizo, A., Amm, O., et al. (2014). Approximate forms of daytime ionospheric conductance. *Journal of Geophysical Research: Space Physics*, *119*, 10,397–10,415. https://doi.org/10.1002/2014ja020665

Knof, H., Vanderslice, J. T., & Mason, E. A. (1964). Interaction energies, charge exchange cross sections, and diffusion cross sections for N^+–N and O^+–O collisions. *Journal of Chemical Physics*, *40*(12), 3548–3553. https://doi.org/10.1063/1.1725050

McGranaghan, R., Knipp, D. J., Solomon, S. C., & Fang, X. H. (2015). A fast, parameterized model of upper atmospheric ionization rates, chemistry, and conductivity. *Journal of Geophysical Research: Space Physics*, *120*, 4936–4949. https://doi.org/10.1002/2015ja021146

Moro, J., Denardini, C. M., Resende, L. C. A., Chen, S. S., & Schuch, N. J. (2016). Influence of uncertainties of the empirical models for inferring the E-region electric fields at the dip equator. *Earth, Planets and Space*, *68*(1), 1–15. https://doi.org/10.1186/s40623-016-0479-0

Picone, J. M., Hedin, A. E., Drob, D. P., & Aikin, A. C. (2002). NRLMSISE-00 empirical model of the atmosphere: Statistical comparisons and scientific issues. *Journal of Geophysical Research*, *107*(A12). https://doi.org/10.1029/2002ja009430

Schunk, R. W. (1977). Mathematical structure of transport-equations for multispecies flows. *Reviews of Geophysics*, *15*(4), 429–445. https://doi.org/10.1029/RG015i004p00429

Schunk, R. W., & Nagy, A. F. (2009). *Ionospheres: Physics, plasma physics, and chemistry*. New York: Cambridge University Press.

Schunk, R. W., & Walker, J. C. G. (1973). Theoretical ion densities in lower ionosphere. *Planetary and Space Science*, *21*(11), 1875–1896. https://doi.org/10.1016/0032-0633(73)90118-9

Thebault, E., Finlay, C. C., Beggan, C. D., Alken, P., Aubert, J., Barrois, O., et al. (2015). International Geomagnetic Reference Field: The 12th generation. *Earth, Planets and Space*, *67*(1), 79. https://doi.org/10.1186/s40623-015-0228-9

World Data Center for Geomagnetism, Kyoto, Nosé, M., Iyemori, T., Sugiura, M., & Kamei, T. (2015). Geomagnetic Dst index. https://doi.org/10.17593/14515-74000